

# Enhanced Electroweak Corrections to Inclusive Boson Fusion Processes at the TeV Scale<sup>\*</sup>

Marcello Ciafaloni  
*Dipartimento di Fisica, Università di Firenze,  
INFN - Sezione di Firenze, and CERN, Geneva  
E-mail: ciafaloni@fi.infn.it*

Paolo Ciafaloni  
*INFN - Sezione di Lecce,  
Via per Arnesano, I-73100 Lecce, Italy  
E-mail: Paolo.Ciafaloni@le.infn.it*

Denis Comelli  
*INFN - Sezione di Ferrara,  
Via Paradiso 12, I-35131 Ferrara, Italy  
E-mail: comelli@fe.infn.it*

## Abstract

Electroweak radiative corrections with double-log enhancements occur in inclusive observables at the TeV scale because of a lack of compensation of virtual corrections with real emission due to the nonabelian (weak isospin) charges of the accelerator beams. Here we evaluate such Bloch-Nordsieck violating corrections in the case of initial longitudinal bosons, which is experimentally provided by boson fusion processes, and is related to the Goldstone-Higgs sector. All four states of this sector are involved in the group structure of the corrections, and cause in particular a novel double log effect due to hypercharge mixing in the longitudinal states. We study both the light- and the heavy-Higgs cases, and we analyze the symmetry breaking pattern of the corrections. The latter turn out to be pretty large, in the 5-10 % range, and show an interesting Higgs mass dependence, even for processes without Higgs boson in the final state.

arXiv:hep-ph/0103316v1 29 Mar 2001

---

<sup>\*</sup>Work supported in part by EU QCDNET contract FMRX-CT98-0194 and by MURST (Italy).

# 1 Introduction

Recent developments [1]-[9] in the treatment of EW radiative corrections at high energies have brought attention to the fact [7, 8] that double-log enhancements of infrared/collinear origin are present even in inclusive observables associated to hard processes at the TeV scale. Such enhancements, involving the effective coupling  $\alpha_W \log^2[s/M_W^2]$ , signal the existence of a lack of compensation of the mass singularities associated with the  $M_W^2/s \rightarrow 0$  limit, due to the non abelian weak-isospin charge of the initial states (that is, electrons or protons) provided by the accelerator. In other words, the Bloch-Norsieck (B-N)theorem, valid for abelian theories, is here violated.

For instance, if we take the example of  $ee^+$  annihilation into hadron jets in a Next Linear Collider (NLC[4]), we found [7] that EW corrections to the total cross section at the TeV threshold are about 5% compared to the strong corrections of 3% and may even be larger if polarization and angular dependence are considered. The simple fact which underlies this surprising result is that the emission of a W boson by the incoming electron changes it into a neutrino whose hadron production cross section off positrons is different from the electron-positron one, and actually happens to be larger than the latter. This causes a lack of compensation with virtual corrections, and thus the double-logarithmic enhancement which turns out to be large in the TeV region. Evaluation of such effects for the next generation colliders is thus needed.

It is amusing to note that the electroweak sector of the standard model is the first instance where such non abelian effect is likely to be seen. In fact, since QCD is in a confined phase, no colored asymptotic states are allowed: as a consequence, colour averaging eliminates the double-log singularities and reduces the violation of collinear factorization to higher twist level [10]. In the EW case, on the other hand, symmetry breaking allows the (non abelian) initial states to be prepared by electromagnetic forces, with ensuing violation of the B-N theorem and of collinear factorization theorems at leading level. We remark elsewhere [12] that a similar effect can occur in broken abelian theories too, due to initial state mixing allowed by symmetry breaking.

The enhancements of EW radiative corrections due to mass singularities were actually first pointed out in exclusive processes at double [1] and single [2] logarithmic level. In view of their size, resummations to all orders are available in the literature [3, 5, 6, 9] but we feel that no well-established treatment of higher order Sudakov logarithms has emerged yet in the broken symmetry case, especially for the subleading ones. Here we stress again the point that the inclusive case is special because it does not depend on the photon effective mass, whose abelian effects cancel out by the B-N theorem. Therefore, exponentiation of leading logarithms can be established in a clearcut way [7].

In a previous paper [8] we have generalized the evaluation of the B-N violating logarithms to the case of initial gauge bosons, by limiting ourselves to transverse polarizations. Gauge bosons close to the mass shell are provided indirectly by the accelerator in the form of boson-fusion processes, whose importance increases with the available energy in comparison with annihilation type processes. We have thus provided a classification of the non canceling logs, which are roughly determined by the Sudakov form factor in the t-channel weak isospin representations occurring in the overlap matrix of the process. The latter are found from the Clebsch Gordan couplings of the t-channel isospin to the weak isospin states of the initial particles, whether doublets (for fermionic initial states) or triplets (for bosonic ones). This classification is here summarized in Sec.2.

In the present paper, we address the problem of longitudinal initial bosons which is special because the longitudinal projection (Sec.3) singles out, by the equivalence theorem [16], the Higgs-Goldstone boson sector, which is sensitive to symmetry breaking and in particular to the Higgs boson mass  $M_H$ .

Since we work in the limit where the hard process invariants are in fixed ratios, and  $s \gg M_W^2$ , we are allowed in the fermionic and transverse boson cases to assume symmetry restoration for the squared matrix elements. In the longitudinal case we need more care: if  $M_H \simeq M_W$  (as hinted at by LEP data [13]), then symmetry restoration is safely assumed for energies above the weak scale (Sec.4). On the other hand, if instead  $M_H \gg M_W$ , in the energy region  $M_H \gg \omega \gg M_W$  the  $SU(2)_L \otimes U(1)_Y$  symmetry is broken by the mass terms, and in general no easy treatment is allowed. For this reason, we shall consider in detail the case of very small  $\tan\theta_W = g'/g$ , because in the  $\theta_W \rightarrow 0$  limit the custodial  $SU(2)_L \otimes SU(2)_R$  symmetry plays a key role [17], and allows in fact a relatively simple treatment of the B-N violating double logs (Sec.5) in the energy region  $M_H \gg \omega \gg M_W$  also.

Finally, we discuss in Sec. 6 the example of jet production by boson fusion, by providing both hard cross section and enhanced radiative corrections for the cases of a light or a heavy Higgs boson. A few details on the collinear cutoffs and on the symmetry breaking pattern are derived in the Appendices.

## 2 Electroweak double Logs in inclusive Processes

EW radiative corrections with leading (double-log) enhancements occur in inclusive observables because of a lack of compensation of infrared logarithms between virtual corrections and real emission. This is due in turn to the fact that initial states in a (non abelian) multiplet may change flavour during emission, and thus interaction probability. Such enhancements, therefore, have been classified [8] according to the weak isospin properties of the initial states (fermions or bosons) and the resulting picture is summarized here.

We consider the structure of “soft” (infrared/collinear) interactions accompanying a hard standard model process  $\{\alpha_I p_I\} \rightarrow \{\alpha_F p_F\}$  where the  $\alpha$ 's and  $p$ 's denote collectively the flavours/colours and momenta of initial and final states. The corresponding S-matrix can be written as an operator in the soft Hilbert space  $\mathcal{H}$ , that collects the states

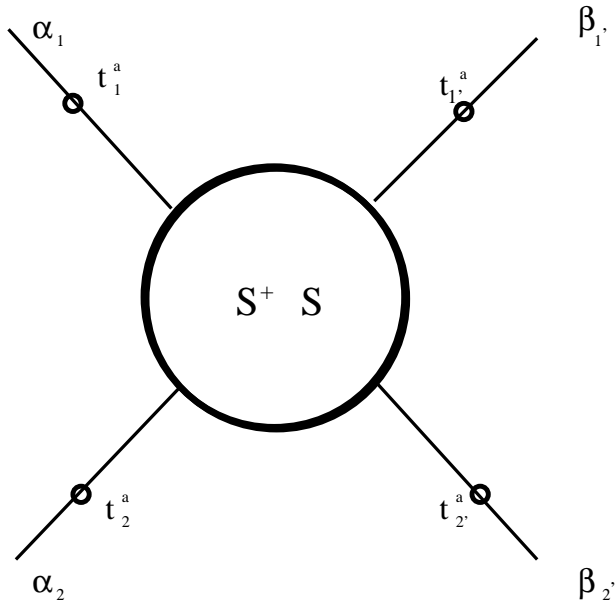


Figure 1: Overlap Matrix

which are almost degenerate with the hard ones, and as a matrix in the hard labels, with form [7]

$$S = \mathcal{U}_{\alpha_F \beta_F}^F(a_s, a_s^\dagger) S_{\beta_F \beta_I}^H(p_F, p_I) \mathcal{U}_{\beta_I \alpha_I}^I(a_s, a_s^\dagger) \quad (1)$$

where  $\mathcal{U}^F$  and  $\mathcal{U}^I$  are operator functionals of the soft emission operators  $a_s, a_s^\dagger$ .

An inclusive measurement on the hard process at hand involves squaring the matrix elements in (1) and summing over the degenerate set  $\Delta(p_F)$  of soft final states. In this procedure, the final state interaction operators  $\mathcal{U}^F$  cancel out by unitarity, so that the relevant quantity is the overlap matrix (Fig. 1)

$$\mathcal{O}_{\beta_I \alpha_I} = {}_S \langle 0 | \mathcal{U}_{\beta_I \beta_I'}^{I\dagger} (S^{H\dagger} S^H)_{\beta_I' \alpha_I'} \mathcal{U}_{\alpha_I' \alpha_I}^I | 0 \rangle_S \quad (2)$$

where  $|0\rangle_S$  denotes the state without soft quanta, as is appropriate for the initial state. It is also convenient to define the hard (tree-level) overlap matrix  $\mathcal{O}^H = S^{H\dagger} S^H$ , which corresponds to eq. (2) if soft radiative corrections are turned off.

Note that physical cross sections of initial particles which are eigenstates of flavours (weak isospin, charge, etc...) involve diagonal overlap matrix elements only. However, off diagonal elements ( $\beta_I \neq \alpha_I$ ) are also relevant in the case of mixing (as for the  $\gamma$  and  $Z$  mass eigenstates) and in order to describe radiative corrections. For this reason we consider a general label assignment in eq. (2).

The factorization of soft operators assumed in eqs. (1) and (2) is typical of a double log treatment, in which collinear singularities are considered in the soft limit, and makes it clear that the B-N violating double logs are due to the initial state interaction. Generalization to subleading EW logarithms requires instead a critical revision of the collinear factorization statements which are valid for QCD.

In order to explicitly evaluate the inclusive double logs, we have used [7] the method of asymptotic dynamics [11] which builds up the  $\mathcal{U}$ -operators in (1) in terms of an effective large-time Hamiltonian, that is constructed in turn by an iterative method to all orders in the gauge couplings. At leading double log level, and in the high energy limit  $s \gg M_W^2 \simeq M_Z^2 \equiv M^2$ , the key ingredient of the asymptotic Hamiltonian is the eikonal soft-boson emission current [11]

$$J^{\mu a}(k) = g \sum_i \mathbf{T}_i^a \frac{p_i^\mu}{p_i \cdot k}, \quad J^{\mu 0}(k) = g' \sum_i y_i \frac{p_i^\mu}{p_i \cdot k} \quad (3)$$

which describes the emission of the gauge bosons eigenstates  $A^{\mu a}, A^{\mu 0}$  ( $a=1,2,3$ ) of momentum  $k$  off the fast charges  $p_i^\mu$  of energy  $E_i \sim \sqrt{s}$  in the soft boson energy region  $\sqrt{s} \gg \omega_k \gg M$ .

Since we work in the high energy fixed angle limit for the hard process, we can assume that the  $SU(2)_L \otimes U(1)_Y$  symmetry is restored in the squared matrix elements for  $\sqrt{s} \gg M$ . Furthermore, since the inclusive double-logs induced by the e.m. charge  $Q$  cancel out by the B-N theorem for abelian theories, there is no net effect from the energy region  $\omega_k < M$  and we can work with only one cutoff

$$\Theta_W = \theta(2p \cdot k - M^2) \quad (4)$$

and with unmixed indices  $(a,0)$  in eq. (3).

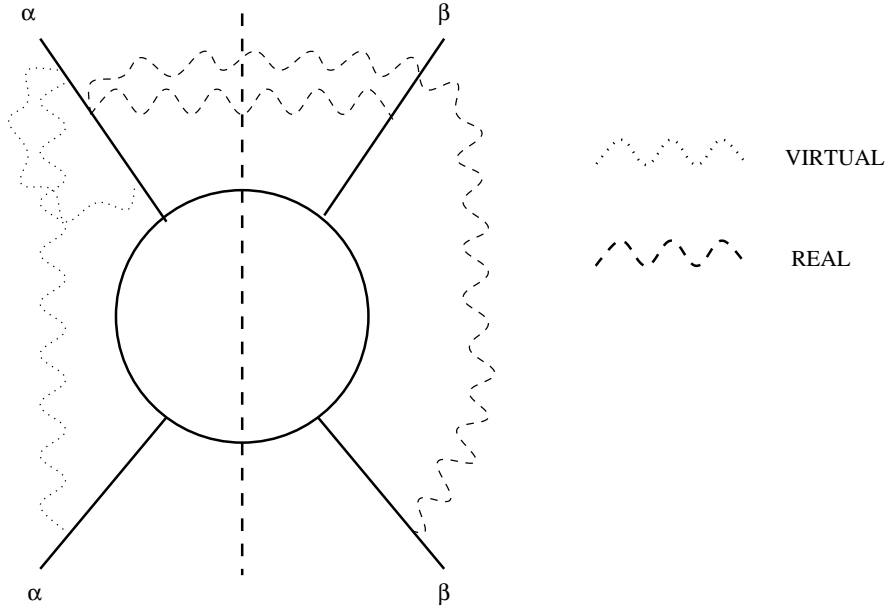


Figure 2: One loop Dressing of the Overlap Matrix

The isospin  $\mathbf{T}^a$  and hypercharge  $y$  operators in eq. (3) act on the flavour indices  $\alpha_I \equiv (\alpha_1 \alpha_2)$  of the (two) initial particles, which are doubled, because of the square, in the overlap matrix  $\mathcal{O}_{\beta_1\beta_2,\alpha_1\alpha_2}$ . Because of the complex conjugation in the square, we shall normally use the representations  $\mathbf{T}$  ( $-\mathbf{T}^T$ ) for doublets on the  $\alpha$ -indices and antidoublets on the  $\beta$ -indices (antidoublets on the  $\alpha$ -indices and doublets on the  $\beta$ -indices), with the identifications

$$\langle \beta_1\beta_2 | \mathcal{O}^{(s)} | \alpha_1\alpha_2 \rangle = \langle \bar{\alpha}_2\bar{\beta}_2 | \mathcal{O}^{(t)} | \alpha_1\bar{\beta}_1 \rangle = \langle \mathcal{O} | \bar{\beta}_1\bar{\beta}_2\alpha_1\alpha_2 \rangle \quad (5)$$

where the bars denote the conjugate representation and the overlap matrix in the first and the second case is decomposed along the  $s$  and  $t$  channel flavour structure.

Restoration of gauge symmetry means that the gauge charges are conserved, i.e.,

$$\mathcal{O}(\sum_i \mathbf{T}_i^a) = \mathcal{O}(\sum_i y_i) = 0, \quad (s \gg M^2) \quad (6)$$

and, as a consequence, the eikonal current (3) is conserved too

$$\mathcal{O} J^{\mu A}(k) k_\mu = 0 \quad (A = (a, 0)) \quad (7)$$

Residual effects of symmetry breaking come, of course, from the weak scale cutoff  $M$ , and from the fact that initial particles may be mixed, being a superposition of different isospin or hypercharge eigenstates. By taking into account soft emission off the legs  $\alpha_1$ ,  $\beta_1$  (with momentum  $p_1$ ) and  $\alpha_2$ ,  $\beta_2$  (with momentum  $p_2$ ) the eikonal current for the overlap matrix becomes, by the gauge charge conservation (6):

$$J^{\mu a}(k) = g \left( \frac{p_1^\mu}{p_1 \cdot k} - \frac{p_2^\mu}{p_2 \cdot k} \right) \mathbf{T}_L^a, \quad J^{\mu 0}(k) = g' \left( \frac{p_1^\mu}{p_1 \cdot k} - \frac{p_2^\mu}{p_2 \cdot k} \right) Y \quad (8)$$

where  $\mathbf{T}_L^a = \mathbf{T}_1^a + \mathbf{T}_{1'}^a$  ( $Y = y_1 + y_{1'}$ ) denotes the total t-channel isospin (hypercharge). For initial states with definite hypercharge ( $y_1 = -y_{1'}$  and  $y_2 = -y_{2'}$ ) we can set  $Y = 0$ . (But see sec.4 for a relevant example with  $Y \neq 0$ ).

Radiative corrections to the hard overlap matrix (Fig.2) come from virtual contributions (connecting two  $\alpha$ -indices or two  $\beta$ -indices) and from real emission (connecting an  $\alpha$ -index with a  $\beta$ -index). A simple counting shows that a soft-boson loop contributes the eikonal radiation factor

$$\frac{1}{2} (J^a(k))^2 = -g^2 \frac{p_1 \cdot p_2}{(p_1 \cdot k)(p_2 \cdot k)} \mathbf{T}_L^2 \Theta_W \quad (9)$$

integrated over the phase space of the (on shell) soft boson.

The leading asymptotic hamiltonian is then found by defining an evolution variable which is conjugated to the asymptotic time and by slicing the  $k$  phase space accordingly [11]:

$$\mathcal{H}(\tau) = \frac{g^2}{(2\pi)^3} \int \frac{d^3k}{2\omega} \delta(\tau - \tau(k)) \frac{p_1 \cdot p_2}{(p_1 \cdot k)(p_2 \cdot k)} \mathbf{T}_L^2 \Theta_W \equiv \mathbf{T}_L^2 \dot{\mathcal{L}}_W(\tau) \quad (10)$$

In general, depending on the choice of  $\tau$  whether energy [11] or emission angle [14] or  $k_T$  variable [15], higher order terms in the effective Hamiltonian may be not negligible. Here we stress the point that the present problem is commutative,  $\mathcal{H}(\tau)$  being proportional to  $\mathbf{T}_L^2$  at all values of  $\tau$ , and thus any definition of  $\tau$  will provide the same result, which is path ordering independent. By  $\tau$  integration we find in fact the Sudakov factor

$$S(s, M_W^2) = P e^{-\int d\tau \mathcal{H}(\tau)} = e^{-\mathbf{L}(s, M^2) \mathbf{T}_L^2} \quad (11)$$

where we have set  $\mathbf{L}_W \equiv \mathbf{L}(s, M^2) \equiv \frac{\alpha_W}{4\pi} \log^2 \frac{s}{M^2}$ , which depends on the casimir  $\mathbf{T}_L^2$  of the total t-channel weak isospin of the problem. Because of gauge symmetry, the hard overlap matrix  $\mathcal{O}_H$  has the form of a sum of projectors of definite (t-channel)  $SU(2) \otimes U(1)$  quantum numbers. It is then straightforward to find the resummed expression for  $\mathcal{O}$ :

$$\mathcal{O}_H = \sum_{t_L} C_{t_L} P_{t_L} \quad \mathcal{O} = e^{-\mathbf{L}(s, M^2) \mathbf{T}_L^2} \mathcal{O}_H = \sum_{t_L} C_{t_L} e^{-\mathbf{L}(s, M^2) t_L(t_L+1)} P_{t_L} \quad (12)$$

The inclusive double logs are thus found for a generic initial state by the following steps:

- First, choose an inclusive hard process which is flavour blind (for instance  $e^-e^+ \rightarrow$  hadronic jets, or flavoured jets, summed over flavour charges).
- Then, calculate the hard overlap matrix and its couplings to t-channel isospin.
- Finally, get the radiative corrections by the weights (11) on each isospin state.

We found [8] by this procedure the following classification.

## 2.1 Fermionic Initial States

This is the most interesting case, which includes electron, muon, and proton colliders above the TeV scale.

Since left-handed fermions have  $t_L = 1/2$ , we should consider doublet scattering for both the  $ff$  (which is equal to  $\bar{f}\bar{f}$ ) and  $f\bar{f}$  (equal to  $\bar{f}f$ ) cases. Isospin and CP conservation provides the constraints

$$\sigma_{11} = \sigma_{22} = \sigma_{\bar{1}\bar{1}} = \sigma_{\bar{2}\bar{2}} \quad \sigma_{1\bar{1}} = \sigma_{2\bar{2}} \quad \sigma_{1\bar{2}} = \sigma_{\bar{1}2} \quad (13)$$

so that there are only four independent cross sections, e.g.,  $\sigma_{12}$ ,  $\sigma_{22}$  in the  $ff$  case, and  $\sigma_{1\bar{2}}$ ,  $\sigma_{2\bar{2}}$  in the  $f\bar{f}$  one.

On the other hand, the t-channel states  $|\alpha_1 \bar{\beta}_1\rangle$  occurring in eq. (5) give rise to  $\mathbf{T}_L = 0, 1$  for both the  $ff$  and  $f\bar{f}$  cases, thus providing again four independent coefficients [8]:

$$\mathcal{O}_{ff} = C_0 P_0 + C_1 P_1 \quad \mathcal{O}_{f\bar{f}} = \bar{C}_0 \bar{P}_0 + \bar{C}_1 \bar{P}_1 \quad (14)$$

Expressions for the resummed cross sections can be directly obtained by projecting eq. (12) on the subset of the states appearing in the projectors that, having  $t_L^3 = 0$ , correspond to physical cross sections\*. There are two such states in the case at hand, providing the equations:

$$\langle ii^* | \mathcal{O} | t_L = 0, t_L^3 = 0 \rangle = \langle ii^* | \mathcal{O}^H | t_L = 0, t_L^3 = 0 \rangle \quad \langle ii^* | \mathcal{O} | t_L = 1, t_L^3 = 0 \rangle = \langle ii^* | \mathcal{O}^H | t_L = 1, t_L^3 = 0 \rangle e^{-2\mathbf{L}_W} \quad (15)$$

where  $i = 1, 2, \bar{1}, \bar{2}$  label the initial states on leg 1 and 1' in Fig. 1. Namely, we find:

- The singlet  $\mathbf{T}_L = 0$  state

$$\frac{1}{\sqrt{2}} (|1\bar{2}\rangle + |2\bar{1}\rangle) = \frac{1}{\sqrt{2}} (|11^*\rangle + |22^*\rangle) \quad (16)$$

corresponding to the average cross sections

$$\frac{1}{2} (\sigma_{12} + \sigma_{22}), \quad \frac{1}{2} (\sigma_{1\bar{2}} + \sigma_{2\bar{2}}) \quad (17)$$

- The triplet  $\mathbf{T}_L = 1$  states whose  $\mathbf{T}_L^3 = 0$  component is

$$-\frac{1}{\sqrt{2}} (|1\bar{2}\rangle + |2\bar{1}\rangle) = \frac{1}{\sqrt{2}} (|11^*\rangle - |22^*\rangle) \quad (18)$$

corresponding to the cross-section differences

$$\sigma_{12} - \sigma_{22}, \quad \sigma_{1\bar{2}} - \sigma_{2\bar{2}} \quad (19)$$

By eq. (15), the average cross section has no radiative corrections, while the difference is suppressed by the form factor in the adjoint representation, e.g.,

$$\sigma_{\nu e^+} - \sigma_{e^- e^+} = (\sigma_{\nu e^+}^H - \sigma_{e^- e^+}^H) e^{-2\mathbf{L}_W} \quad (20)$$

This leads to corrections  $\Delta\sigma_{e^-e^+}/\sigma_{e^-e^+}^H$  of order 5% for  $e^-e^+$  annihilation into hadrons at the TeV threshold.

\*The elements of the overlap matrix corresponding to physical cross section always involve a given particle on leg 2 and its own antiparticle on leg 2' in fig. 1, and have thus all t-channel additive quantum numbers set to 0.

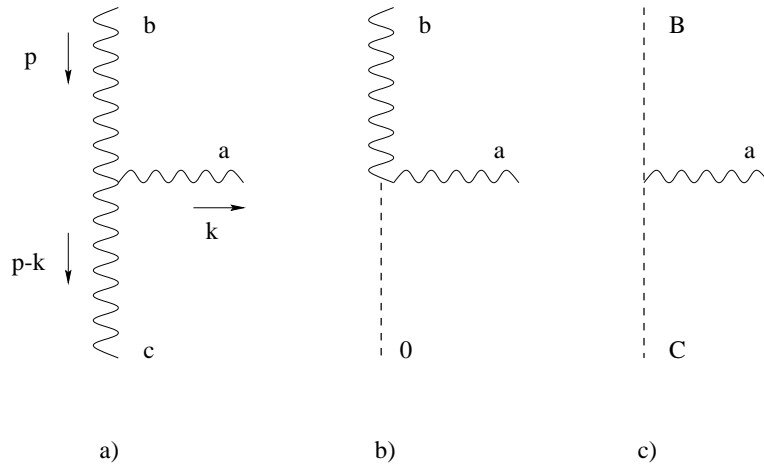


Figure 3: Leading Eikonal Vertices in the Longitudinal (a,b) and Scalar (c) Sector

## 2.2 Transverse Bosons

This case is needed in order to treat boson-fusion processes, in which nearly on-shell gauge bosons are exchanged. It must be supplemented by the longitudinal case to the studied below, which is favoured at very high energies.

Since transverse bosons behave as genuine isospin triplets, it is straightforward to derive the isospin conservation constraints:

$$\sigma_{++} = \sigma_{--}, \quad \sigma_{3+} = \sigma_{3-}, \quad \sigma_{33} = \sigma_{++} + \sigma_{--} - \sigma_{3+} \quad (21)$$

so that only three independent cross sections are left

$$\sigma_\alpha = \sigma_{\alpha+} \quad (\alpha = +, 3, -) \quad (22)$$

Correspondingly, the t-channel isospin can take the values  $\mathbf{T}_L = 0, 1, 2$ , leading to three projectors and three independent coefficients.

The  $|\alpha_1 \bar{\beta}_1\rangle$  states diagonalizing such projectors are:

- The singlet state

$$\frac{1}{\sqrt{2}}(|+-\rangle + |-+\rangle + |33\rangle) \quad (23)$$

corresponding to the cross section average  $\frac{1}{3} \sum_\alpha \sigma_\alpha$ ;

- Three  $\mathbf{T}_L = 1$  states, whose  $\mathbf{T}_L^3 = 0$  component is

$$\frac{1}{\sqrt{2}}(|+-\rangle - |-+\rangle) \quad (24)$$

corresponding to the difference  $\sigma_+ - \sigma_-$ ;

- Five  $\mathbf{T}_L = 2$  states, whose  $\mathbf{T}_L^3 = 0$  component is

$$\frac{1}{\sqrt{6}}(|+-\rangle + |-+\rangle - 2|33\rangle) \quad (25)$$

corresponding to the cross section combination

$$\sigma_+ + \sigma_- - 2\sigma_3 \quad (26)$$

Due to the weights (11), the average cross section has no radiative corrections, the difference  $\sigma_+ - \sigma_-$  is damped by the form factor in the adjoint representation  $\sim e^{-2\mathbf{L}w}$ , much as in eq. (20), and the combination (26) is damped even more strongly, by the form factor in the  $\mathbf{T}_L = 2$  representation  $\sim e^{-6\mathbf{L}w}$ .

## 3 Soft Emission in the longitudinal Sector and Equivalence Theorem

It is well known that, in the high energy limit longitudinal polarizations are of type  $\epsilon_L^\mu \simeq p^\mu/M + O(M/E)$ , and therefore longitudinal boson amplitudes  $A_\lambda^a$  are related to the Goldstone bosons ones by the equivalence theorem [16]

$$\frac{p^\lambda}{M} \mathcal{M}_\lambda^a(p; \dots) \simeq i\mathcal{M}(\varphi^a(p); \dots), \quad p^2 \simeq M^2 \quad (27)$$

where  $a = 1, 2, 3$  labels the  $SU(2)_L$  vector boson indices and the remaining momentum and flavour indices of the amplitudes have been dropped. <sup>†</sup> Therefore, the soft emission properties of the longitudinal bosons are related to the ones of Goldstone bosons, which are coupled to the Higgs boson in the scalar sector. This shows that the dynamics of soft boson emission involves actually four real states ( $\varphi^a$ ,  $h$ ) or the Higgs doublet and its conjugate. We shall see that depending on the mass parameters of the problem, the doublet/antidoublet or triplet/scalar description may be best suited, both in general being needed.

In order to better understand this point, let us consider the emission of a soft boson with isospin index  $a$ , Lorentz indices  $\mu$ , and momentum  $k$  off an energetic vector boson ( $\epsilon_\lambda(p)$ ) via the three boson coupling. The amplitude (Fig.3a) is proportional to

$$\epsilon_\lambda(p)\Gamma^{\lambda\mu\nu}(p, k) = \epsilon_\lambda(p)[g^{\lambda\nu}(2p+k)^\mu - g^{\mu\nu}(p+2k)^\lambda] \quad (28)$$

$$- g^{\lambda\mu}(p-k)^\nu] \simeq 2p^\mu \epsilon^\nu(p) - \epsilon^\mu(p) p^\nu + O(k) \quad (29)$$

where use has been made of the condition  $\epsilon(p) \cdot p = 0$ . By taking into account the denominator and isospin factors, we then obtain a generalized eikonal emission amplitude

$$\langle \mathcal{M}(b, \epsilon(p); \dots) | a, \mu, k \rangle \simeq i g \epsilon_{bac} \left[ \mathcal{M}(c, \epsilon(p+k); \dots) \frac{p^\mu}{p \cdot k} - \frac{M}{2p \cdot k} \epsilon^\mu(p) \mathcal{M}(c, \epsilon_L(p+k); \dots) \right] \quad (30)$$

which differs from the customary one of the unbroken theories by the second term in square brackets, which is purely longitudinal. If  $\epsilon(p)$  is a transverse polarization, the second term is of order  $\frac{M}{E}$  with respect to the first one, and is thus subleading. On the other hand, if  $\epsilon(p) \sim p/M + O(M/E)$  is the longitudinal polarization, then the latter term cancels one half the ‘‘leading’’ term, and leads to a factorized eikonal emission current off longitudinal bosons:

$$\langle \mathcal{M}(b, \epsilon_L(p); \dots) | a, \mu, k \rangle \simeq i \frac{g}{2} \epsilon_{bac} \left[ \mathcal{M}(c, \epsilon_L(p+k); \dots) \frac{p^\mu}{p \cdot k} (1 + O(\frac{\omega}{E})) \right] \quad (31)$$

Note the factor of  $\frac{1}{2}$ , relative to the normal eikonal factorization theorem for transverse polarizations.

The amplitude (31) is not however, the only possible contribution to soft boson emission, which can occur via a Higgs boson also (Fig.3b). Taking into account the weak scale dependence properly, one finds again the factorized eikonal current, with a Higgs contribution on the r.h.s.:

$$\langle \mathcal{M}(b, \epsilon_L(p); \dots) | a, \mu, k \rangle \simeq \frac{g}{2} \frac{p^\mu}{p \cdot k} [i \epsilon_{bac} \mathcal{M}(c, \epsilon_L(p+k); \dots) - i \delta_{ab} \mathcal{M}(h(p+k); \dots)] \quad (32)$$

Since the Higgs boson can occur as a final state as well (Fig.3c) it is convenient to generalize eq. (32) in matrix form on the boson indices  $B = (b, 0) \equiv (\varphi_a, h)$ , as follows:

$$\langle \mathcal{M}(\varphi^B(p); \dots) | a, \mu, k \rangle \simeq g \frac{p^\mu}{p \cdot k} (\mathbf{T}_L^a)_{BC} \mathcal{M}(\varphi^C(p+k); \dots) \quad (33)$$

by thus introducing the weak isospin matrix in the  $(\varphi^a, h)$  basis

$$\mathbf{T}_L^a = \frac{1}{2} \begin{pmatrix} i \epsilon_{bac} & -i \delta_{ab} \\ i \delta_{ac} & 0 \end{pmatrix} \equiv \frac{1}{2} (T_V^a + T_h^a) \quad (34)$$

where  $(T_V^a)_{bc} = i \epsilon_{bac}$ . Similarly one can define the eikonal emission current of the  $B_\mu \equiv A_\mu^0$  boson in the form:

$$\langle \mathcal{M}(\varphi^B(p); \dots) | 0, \mu, k \rangle \simeq g' \frac{p^\mu}{p \cdot k} Y_{BC} \mathcal{M}(\varphi^C(p+k); \dots) \quad (35)$$

where

$$Y = \frac{1}{2} (T_V^3 - T_h^3) \quad (36)$$

is the hypercharge matrix in this sector. Eqs. (34) and (36) are the basis for our treatment of radiative corrections in the following.

It is important to realize that the gauge generators (34) and (36) have a simple structure within the custodial symmetry group  $SU(2)_L \otimes SU(2)_R$  [17]. In fact it is straightforward to check that  $T_V$  and  $T_h$  in eq. (34) satisfy the algebra of the  $O(4)$  group

$$[T_V^a, T_V^b] = i \epsilon^{abc} T_V^c, \quad [T_V^a, T_h^b] = i \epsilon^{abc} T_h^c, \quad [T_h^a, T_h^b] = i \epsilon^{abc} T_V^c, \quad (37)$$

<sup>†</sup> Strictly speaking, we should have written eq. (27) for the Z-boson instead of its  $A^3$  component  $\frac{p^\lambda}{M_Z} \mathcal{M}_\lambda^{ZL}(p; \dots) \simeq \mathcal{M}(\varphi^3(p); \dots)$ . But using the relation  $M_Z = M_W/c_W$  and electromagnetic current conservation provides eq. (27) close to the vector boson mass shell

As a consequence, the  $SU(2)_L$  ( $SU(2)_R$ ) generators  $\mathbf{T}_L^a$  ( $\mathbf{T}_R^a$ ) are provided by

$$\mathbf{T}_L^a = \frac{1}{2}(T_V^a + T_h^a), \quad \mathbf{T}_R^a = \frac{1}{2}(T_V^a - T_h^a) \quad (38)$$

So that  $[\mathbf{T}_L^a, \mathbf{T}_R^b] = 0$  and  $Y = \mathbf{T}_R^3$ . In this language the basis  $(\varphi^a, h)$  is just the  $(\frac{1}{2}, \frac{1}{2})$  representation of the group  $O(4) \sim SU(2)_L \otimes SU(2)_R$ , characterized by  $\mathbf{T}_L^2 = \mathbf{T}_R^2 = 3/4$ , and the matrices (34) and (36) refer to the 4-vector representation.

Of course, the same type of eikonal current (33) arises by direct study of the Goldstone-Higgs sector and of their couplings to soft bosons, as expected from the equivalence theorem (Fig.3c). The longitudinal projection just provided helps clarifying some aspects of the problem, in particular the factor  $\frac{1}{2}$  occurring in (34), and the occurrence of four states associated with the longitudinal bosons. It is sometimes useful to arrange such four states of the  $(\frac{1}{2}, \frac{1}{2})$  representation in the complex form of the doublet/antidoublet matrix

$$\Phi = \frac{1}{\sqrt{2}}(h + i\tau_a\varphi_a) = \begin{pmatrix} \varphi_0 & i\varphi_+ \\ i\varphi_- & \varphi_0^* \end{pmatrix} = \frac{1}{\sqrt{2}} \begin{pmatrix} h + i\varphi_3 & \varphi_2 + i\varphi_1 \\ -\varphi_2 + i\varphi_1 & h - i\varphi_3 \end{pmatrix} = \begin{pmatrix} \bar{1} & 1 \\ \bar{2} & 2 \end{pmatrix} \quad (39)$$

which transforms as  $\Phi \rightarrow U_L \Phi U_R^\dagger$  under the  $SU(2)_L \otimes SU(2)_R$  group. The indices 1, 2,  $\bar{1}$ ,  $\bar{2}$  here refer to the transformation properties under  $SU(2)_L$ .

## 4 Radiative Corrections in the light Higgs case

For Higgs bosons and vector bosons nearly degenerate, the gauge symmetry of the squared matrix elements is restored in the full high-energy region  $\omega \gg M = M_W \simeq M_H$  (the common weak scale), while the photon scale plays no role because of the B-N theorem for QED. Therefore, we can assume  $SU(2)_L \otimes U(1)_Y$  symmetry for both the hard overlap matrix and for enhanced radiative corrections, as already discussed in sec.2.

Since the longitudinal bosons are related to the Higgs doublets by the equivalence theorem (sec.3), and the latter have  $t_L = 1/2$ , it would seem that we are in the same case as that of fermion and antifermion doublets. However, a peculiarity of the longitudinal/Higgs sector is the fact that the physical Higgs boson is by itself a manifestation of (low-energy) symmetry breaking, being a coherent superposition (see (39))

$$|h\rangle = \frac{|\varphi_0\rangle + |\varphi_0^*\rangle}{\sqrt{2}} = \frac{|\bar{1}\rangle + |2\rangle}{\sqrt{2}} \quad (40)$$

of doublet states of opposite hypercharge. Since the state (40) has no definite hypercharge, it happens that overlap matrix elements having non vanishing t-channel hypercharge  $Y = \pm 1$  occur in physical cross sections initiated by neutral states, besides the normal ones with  $Y = 0$ .

The fact above has no counterpart in the light fermion case <sup>‡</sup> because it is not possible to prepare a coherent superposition of a fermion and of its antifermion, due to exact fermion number conservation. On the other hand, a similar phenomenon occurs in the customary case of  $B_\mu - W_\mu^3$  mixing yielding  $\gamma$  and  $Z$  mass eigenstates, as already discussed in ref.[8]. In the latter case the mixing is nonabelian, involving  $t_L = 1$  and  $t_L = 0$  states, while in the Higgs case the mixing is abelian, involving  $y = \pm 1/2$  hypercharge states. A peculiar consequence of this fact is that violation of B-N theorem can occur in broken abelian theories too [12].

By using the definitions (39), the gauge symmetry constraints (13) in the longitudinal /Higgs sector can be written as follows:

$$\sigma_{--} = \sigma_{++}, \quad ; \quad \sigma_{+3} = \sigma_{-3} = \sigma_{+h} = \sigma_{-h} \quad (41)$$

In the purely neutral sector we find, on the other hand, the mixing phenomenon, in the form:

$$\begin{aligned} \sigma_{33} = \sigma_{hh} &= \frac{1}{2}(\sigma_{++} + \sigma_{+-}) + \text{Re}(\mathcal{O}) \\ \sigma_{3h} &= \frac{1}{2}(\sigma_{++} + \sigma_{+-}) - \text{Re}(\mathcal{O}) \end{aligned} \quad (42)$$

where  $\mathcal{O} \equiv \mathcal{O}(\varphi_0\varphi_0^* \rightarrow \varphi_0^*\varphi_0)$  and its conjugate denote the  $Y = 1$  and  $Y = -1$  overlap matrix elements mentioned before.

It is then convenient to refer to a fixed target (the + state, say) in order to enumerate the independent cross sections. Due to eqs. (41) we find at once three of them

$$\sigma_{++}, \sigma_{-+}, \sigma_{3+} \quad (43)$$

<sup>‡</sup>Note however that mixing occurs in the case of transversely polarized fermions, which are indeed a superposition of states of opposite chirality, and of different gauge quantum numbers [12]



similarly to the transverse polarization case and in addition to the neutral overlap  $Re\mathcal{O}$  just defined. Finally, we also need another off diagonal matrix element

$$I \equiv \text{Im}\mathcal{O}_{h3} \equiv \text{Im}(\mathcal{O}_{3+\rightarrow h+}) = \frac{1}{2}(\sigma_{0+} - \sigma_{0*+}) \quad (44)$$

in order to express all possible initial state dependences. All these five quantities, except  $Re\mathcal{O}$ , have  $Y = 0$  in the t-channel.

We shall now compute the enhanced (B-N violating) radiative corrections to the observables (42) and (43). Following our method (sec.2), we have to (i) define the hard process and the inclusive (flavour blind) observable we are interested in (ii) derive the lowest order (tree level) hard overlap matrix  $\mathcal{O}_{\beta_1\beta_2,\alpha_1\alpha_2}^H$  and (iii) derive the effective hamiltonian describing the enhanced radiative corrections, for the given initial state configuration.

Symmetry considerations restrict the hard overlap matrix, according to the possible t-channel quantum numbers whose eigenstates are constructed out of the  $|\alpha_1\bar{\beta}_1\rangle$  states defined before. In the longitudinal/Higgs sector  $\alpha_1$  and  $\beta_1$  span the four states of the  $(1/2, 1/2)$  representation, so that the  $|\alpha_1\bar{\beta}_1\rangle$  states can be classified as follows (see Appendix B for the explicit expressions):

- Eight ( $Y = 0$ ) states, which can be grouped according to left isospin representation, and  $CP = \pm 1$  eigenvalues. We find thus the projectors:

$$T^{CP}(m) = 0^-(1), \quad 1^-(3), \quad 0^+(1); \quad 1^+(3), \quad (45)$$

corresponding to four independent coefficients, each with the multiplicity  $m$  of states in parenthesis. Such four projectors are in close correspondence with the ones for the fermionic doublets discussed in sec 2. Note that the  $CP$  eigenstates  $+1$  ( $-1$ ) are just symmetric (antisymmetric) under doublet-antidoublet interchange.

- Four ( $Y = 1$ ) and four ( $Y = -1$ ) states, which are interchanged by  $CP$  and must thus be degenerate, which can be classified according to left isospin representation:

$$T(m) = 0(2), \quad 1(6) \quad (46)$$

corresponding to two more independent coefficients.

Actually only five out of the overall six independent coefficients are coupled to the observables enumerated in eq. (43) and (44), (the one corresponding to  $\mathbf{T}_L = 0$  and  $Y = Q = \pm 1$  being decoupled from physical states by the e.m. charge superselection rule).

The effective hamiltonian describing radiative corrections is found by exactly the same method as in sec 2, with the important difference that now we can have a non vanishing t-channel hypercharge, and we thus obtain

$$\mathcal{H}(\tau) = \dot{\mathbf{L}}_W(\tau)(\mathbf{T}_L^2 + tg^2\theta_W Y^2) \quad (47)$$

from which the t-channel Sudakov factors

$$S(\mathbf{T}_L, Y) = e^{-\mathbf{L}_W(s, M_W^2)(\mathbf{T}_L^2 + tg^2\theta_W Y^2)} \quad (48)$$

are found for each one of the states (45) and (46).

In order to assign the Sudakov weights to the observables (41) and (44) we need to relate them to the explicit form of the states which diagonalize the projectors (45) and (46). A direct construction of them is obtained from their classification according the  $SU(2)_L \otimes SU(2)_R$  group; this construction is explicitly worked out in Appendix B, From the direct product of two  $(\frac{1}{2}, \frac{1}{2})$  representations we obtain the following representations

$$\left(\frac{1}{2}, \frac{1}{2}\right) \otimes \left(\frac{1}{2}, \frac{1}{2}\right) = (0, 0) \oplus (0, 1) \oplus (1, 0) \oplus (1, 1) \quad (49)$$

which are related to those in (45) and (46) as follows:

- The state  $(0, 0)$  is the  $0^-$  state and corresponds to the average cross section

$$\sigma_+ + \sigma_- + \sigma_0 + \sigma_{\bar{0}} = \sigma_+ + \sigma_- + \sigma_3 + \sigma_{\bar{3}} = \sigma_+ + \sigma_- + 2\sigma_3 \equiv \Sigma + 2\sigma_3 \quad (50)$$

where we introduce the notation  $\sigma_\alpha \equiv \sigma_{\alpha+}$  in which the  $+$  target is understood. The identification (50) is obtained by the explicit construction

$$|0; 0\rangle = \frac{1}{2}(-|1\bar{2}\rangle + |2\bar{1}\rangle + |\bar{1}2\rangle - |\bar{2}1\rangle) = \frac{1}{2}(|+-\rangle + |-+\rangle + |0\bar{0}\rangle + |\bar{0}0\rangle) = \quad (51)$$

$$\frac{1}{2}(|+-\rangle + |-+\rangle + |33\rangle + |hh\rangle) \quad (52)$$

which has, by inspection,  $t_L = t_R = 0$ , and is also antisymmetric into the doublet indices interchange  $i \leftrightarrow \bar{i}$ . Eq.(50) corresponds to the matrix element  $\langle +- | \mathcal{O} | 0; 0 \rangle$ .

- The three states  $(0, 1)$  are split according to the hypercharge  $Y = \mathbf{T}_R^3$  into (i) the two degenerate  $t_L = 0$ ,  $Y = \pm 1$  states in (46) and (ii) the symmetric  $t_L = Y = 0$  state in (45). The latter corresponds to the combination

$$\sigma_+ - \sigma_- + 2 \operatorname{Im} \mathcal{O}_{h3} \equiv \Delta + 2 I, \quad \mathcal{O}_{h3} = \langle h + |\mathcal{O}|3+ \rangle, \quad 0^+ \quad (53)$$

and to the state  $0^+$ , provided by

$$|0; t_R = 1, Y = 0\rangle = \frac{1}{2}(-|1\bar{2}\rangle + |2\bar{1}\rangle - |\bar{1}2\rangle + |\bar{2}1\rangle) = \frac{1}{2}(|+-\rangle - |-+\rangle + |0\bar{0}\rangle - |\bar{0}0\rangle) \quad (54)$$

- The three states  $(1, 0)$  are the antisymmetric  $1^-$  states, whose  $t_L^3 = 0$  term is the only one related to cross-sections, and corresponds to the combination

$$\sigma_+ - \sigma_- - 2 \operatorname{Im} \mathcal{O}_{h3} \equiv \Delta - 2 I, \quad 1^- \quad (55)$$

and to the state

$$|1, t_L^3 = 0; 0\rangle = \frac{1}{2}(-|1\bar{2}\rangle - |2\bar{1}\rangle + |\bar{1}2\rangle + |\bar{2}1\rangle) = \frac{1}{2}(|+-\rangle - |-+\rangle - |0\bar{0}\rangle + |\bar{0}0\rangle) \quad (56)$$

- The nine  $(1, 1)$  states are split, according to the hypercharge quantum number into (i) six degenerate  $t_L = 1$ ,  $Y = \pm 1$  states occurring in (46) and (ii) three  $Y = 0$ ,  $1^+$  states occurring in (45), whose  $t_L^3 = 0$  term corresponds to the cross section

$$\sigma_+ + \sigma_- - \sigma_0 - \sigma_{\bar{0}} = \sigma_+ + \sigma_- - \sigma_3 - \sigma_h = \sigma_+ + \sigma_- - 2\sigma_3 \equiv \Sigma - 2\sigma_3, \quad (1^+) \quad (57)$$

and to the state

$$|1, t_L^3 = 0; 1, t_R^3 = 0\rangle = \frac{1}{2}(-|1\bar{2}\rangle - |2\bar{1}\rangle - |\bar{1}2\rangle - |\bar{2}1\rangle) = \frac{1}{2}(|+-\rangle + |-+\rangle - |0\bar{0}\rangle - |\bar{0}0\rangle) \quad (58)$$

On the other hand, the state corresponding to the overlap  $\mathcal{O}(\varphi_0 \varphi_0^* \rightarrow \varphi_0^* \varphi_0)$  in the neutral sector has  $t_L^3 + t_R^3 = Q = 0$  and corresponds to the states  $|00\rangle$  or  $|\bar{0}\bar{0}\rangle$  in (45). Other states with  $Y \neq 0$  give rise to  $Q \neq 0$  and therefore cannot be coupled to physical cross sections.

The cross-section assignments just provided are summarized in Table 1(a,b).

We are now in a position to provide the Sudakov evolution in eq. (47) for each one of the cross section combinations just introduced. By using the relevant  $(t_L, Y)$  assignments, we find

$$\begin{aligned} \sigma_+ + \sigma_- + 2\sigma_3 &= \Sigma^H + 2\sigma_3^H, & \sigma_h &= \sigma_3 \\ \sigma_+ + \sigma_- - 2\sigma_3 &= (\Sigma^H - 2\sigma_3^H) e^{-2\mathbf{L}_W}, \\ \sigma_+ - \sigma_- + 2I &= \Delta^H + 2I^H, \\ \sigma_+ - \sigma_- - 2I &= (\Delta^H - 2I^H) e^{-2\mathbf{L}_W}, \\ \operatorname{Re} \mathcal{O} &= \operatorname{Re} \mathcal{O}^H e^{-\mathbf{L}_W(2+tg^2\theta_W)}, \\ \sigma_{3h} &= \frac{1}{2}(\sigma_+ + \sigma_-) - \operatorname{Re} \mathcal{O}, \\ \sigma_{33} = \sigma_{hh} &= \frac{1}{2}(\sigma_+ + \sigma_-) + \operatorname{Re} \mathcal{O} \end{aligned} \quad (59)$$

from which all radiative corrections can be derived once the hard (tree level) cross sections are known.

## 5 The heavy Higgs Case and Symmetry Breaking Pattern

If the Higgs mass happens to be much larger than the vector boson mass, then in the energy region  $M_H \gg \omega \gg M_W$  gauge symmetry is broken by the mass spectrum even if the overall energy of the process is  $s \gg M_H^2$ . Therefore, if we want to keep track of the leading powers of all logarithms, whether  $\log[M_H^2/M_W^2]$  or the customary ones  $\log[s/M_W^2]$ , we end up with a process with two mass scales, in which symmetry breaking causes a lack of conservation of the gauge current and therefore requires a more refined treatment of the B-N violation logs and of their scales.

Since we feel that despite recent efforts [9] the direct diagrammatic calculation of higher order Sudakov logarithms in the many scale, broken symmetry case, is not yet fully understood, we prefer to treat here the particular case  $g'/g \rightarrow 0$ , in which the custodial symmetry  $SU(2)_L \otimes SU(2)_R$  of the longitudinal/Higgs sector plays a key role, by providing a conserved current which considerably simplifies the problem. Note in fact that, at tree level and in the high energy limit  $s \gg M_H^2 \gg M_W^2$ , the gauge symmetry is still valid and is actually extended to the full  $SU(2)_L \otimes SU(2)_R$  group in the  $\theta_W \rightarrow 0$  limit. On the other hand, radiative corrections in the energy region  $M_H \gg \omega \gg M_W$  break

the gauge symmetry, but keep the global custodial symmetry  $SU(2)_V \subset SU(2)_L \otimes SU(2)_R$  which then provides the conserved current we are interested in.

In order to understand this point, recall that the infrared/collinear behavior is regulated by the boson emission current (33) where the weak isospin charge is written as the sum of its vector component ( $1/2 T_V^a$ ) and of a Higgs contribution. In order to take into account the mass cutoffs in the denominators, we write the current in eq. (33) in the more precise form

$$J^{a\mu}(k) = g \frac{p^\mu}{p \cdot k} \frac{1}{2} (T_V^a \Theta_W + T_h^a \Theta_H) = g \frac{p^\mu}{p \cdot k} (T_L^a \Theta_H + \frac{1}{2} T_V^a \Theta_W (1 - \Theta_H)) \quad (60)$$

where

$$\Theta_i = \theta(2p \cdot k - M_i^2), \quad i = W, H \quad (61)$$

denote the mass cutoffs.

It is apparent from eq. (60) that the soft boson insertion current is the full gauge current for  $2p \cdot k > M_H^2$ , while it becomes the  $SU(2)_V$  current (with coupling  $g/2$ ) in the region  $M_H^2 > 2p \cdot k > M_W^2$ . Since each current is conserved in the corresponding validity region, the evolution of radiative corrections follows the same pattern as that outlined in sec.2, and the evolution hamiltonian derived from the current (60) becomes

$$\mathcal{H}(\tau) = \dot{\mathbf{L}}_H(\tau) \mathbf{T}_L^2 + \frac{T_V^2}{4} (\dot{\mathbf{L}}_H(\tau) - \dot{\mathbf{L}}_W(\tau)) \quad (62)$$

where the  $\dot{\mathbf{L}}_H(\tau)$ ,  $(\dot{\mathbf{L}}_H(\tau) - \dot{\mathbf{L}}_W(\tau))$  contribution is defined with the phase space slicing in eq. (10), following the cutoff structure  $\Theta_H$ ,  $(\Theta_H - \Theta_W)$  in eq.(60). After  $\tau$ -integration, for  $E > M_H^2/M_W$ , the two exponents turn out to be (Appendix A):

$$\mathbf{L}_W = \frac{\alpha_W}{4\pi} \log^2 \frac{s}{M_W^2} \quad \mathbf{L}_H = \frac{\alpha_W}{4\pi} (\log^2 \frac{s}{M_W^2} - 2 \log^2 \frac{M_H^2}{M_W^2}) \equiv \mathbf{L}_W - 2\mathbf{L}_h \quad (63)$$

Note that, since  $T_V^a = \mathbf{T}_L^a + \mathbf{T}_R^a$ ,  $\mathbf{T}_L^a$  transforms as a vector under  $T_V$  rotations, and therefore  $\mathbf{T}_L^2$  transforms as a scalar, i.e., it is invariant. It follows that the two terms in (62) commute between each other, and therefore  $[\mathcal{H}(\tau), \mathcal{H}(\tau')] = 0$  thus making the Sudakov exponent independent of the type of phase space slicing (whether in  $\omega$  or in  $k_T$ ). By  $\tau$  integration we then obtain

$$S(s, M_H^2, M_W^2) = e^{-\mathbf{T}_L^2 \mathbf{L}_H - \frac{T_V^2}{4} (\mathbf{L}_W - \mathbf{L}_H)} \quad (64)$$

Note finally that the hamiltonian (62) commutes with  $T_V^a$  (but not with  $\mathbf{T}_L^a$ ), so that the overlap matrix radiative corrections are diagonalized by  $SU(2)_V$ , as anticipated before.

In practice, explicit projectors and cross section evolution are constructed as follows. The hard overlap matrix possesses full  $SU(2)_L \otimes SU(2)_R$  symmetry, and therefore is classified directly according to the representation occurring in the direct product (49), corresponding to four independent coefficients. If radiative corrections are turned on, the symmetry is broken to  $SU(2)_V$  and the corresponding states are classified according to the Casimir  $T_V^2$ . Eigenstates of  $T_V^2$  are trivially constructed for the cases

a)  $\mathbf{T}_L^2 = T_V^2 = 0, \quad CP = -1$

b)  $\mathbf{T}_L^2 = 0, \quad T_V^2 = \mathbf{T}_R^2 = 1, \quad CP = +1$

c)  $\mathbf{T}_L^2 = T_V^2 = 1, \quad CP = -1$

discussed before, because they are directly provided by eqs.(51),(54),(56), respectively.

In the case

d)  $\mathbf{T}_L = \mathbf{T}_R = 1$

the degeneracy is resolved by the vector sum  $T_V^a = \mathbf{T}_L^a + \mathbf{T}_R^a$ , so that we can have  $T_V = 0, 1, 2$ . By straightforward algebra (appendix B) we find

d0) The  $\mathbf{T}_L = 1, \quad T_V = 0$  state

$$\begin{aligned} & \frac{1}{\sqrt{3}} (|-\bar{1}\bar{1}\rangle - |22\rangle - \frac{1}{2} (|1\bar{2}\rangle + |2\bar{1}\rangle + |\bar{1}2\rangle + |\bar{2}1\rangle)) = \\ & \frac{1}{2\sqrt{3}} (-2|00\rangle - 2|\bar{0}\bar{0}\rangle + |+-\rangle + |-+\rangle - |0\bar{0}\rangle - |\bar{0}0\rangle) \end{aligned} \quad (65)$$

corresponding to the cross section combination

$$\sigma_+ + \sigma_- + \sigma_3 - 3\sigma_h \quad (66)$$

	$(t_L, t_R)$	$t_L^{CP}$	$Y^2$	$T_V$	Cross Section
a	(0,0)	$0^-$	0	0	$\sigma_+ + \sigma_- + \sigma_3 + \sigma_h$
a	(0,1)	$0^+$	0	1	$\sigma_+ - \sigma_- + 2 Im\mathcal{O}_{h3}$
b, c	(1,0)	$1^-$	0	1	$\sigma_+ - \sigma_- - 2 Im\mathcal{O}_{h3}$
b	(1,1)	$1^+$	0		$\sigma_+ + \sigma_- - \sigma_3 - \sigma_h$
c	(1,1)			2	$\sigma_+ + \sigma_- - 2\sigma_3$
b	(1,1)	1	1		$2 Re\mathcal{O}$
c	(1,1)			0	$\sigma_+ + \sigma_- + \sigma_3 - 3\sigma_h$

Table 1: t-Channel quantum number assignments of various cross section combinations. (a) Invariants, (b)  $SU(2)_L \otimes U(1)_Y$  states ( $M_H \simeq M_W$ ) and (c)  $SU(2)_V$  states ( $M_H \gg M_W$ ). The unphysical  $Q \neq 0$  states have been omitted.

d1) Three  $\mathbf{T}_L = T_V = 1$  states whose  $Q = T_V^3 = 0$  term is

$\frac{1}{i\sqrt{2}}(|\bar{1}\bar{1}\rangle - |22\rangle) = \frac{1}{i\sqrt{2}}(|\bar{0}\bar{0}\rangle - |00\rangle)$  corresponding to an overlap of the type  $Im\mathcal{O}(\varphi_0\varphi_0^* \rightarrow \varphi_0^*\varphi_0)$  which does not occur in physical cross sections.

d2) Five  $\mathbf{T}_L = 1$ ,  $T_V = 2$  states, whose  $T_V^3 = 0$  term is

$$\frac{1}{\sqrt{6}}(|\bar{1}\bar{1}\rangle + |22\rangle - |\bar{1}\bar{2}\rangle - |\bar{2}\bar{1}\rangle - |\bar{1}\bar{2}\rangle - |\bar{2}\bar{1}\rangle) = \frac{1}{\sqrt{6}}(|00\rangle + |\bar{0}\bar{0}\rangle + |+-\rangle + |-+\rangle - |0\bar{0}\rangle - |\bar{0}0\rangle) \quad (67)$$

corresponding to the cross section combination

$$\sigma_+ + \sigma_- - 2\sigma_3 \quad (68)$$

The cross-section assignments just provided are summarized in Table 1(a,c).

Correspondingly, the independent cross sections are  $\sigma_+$ ,  $\sigma_-$ ,  $\sigma_3$ ,  $\sigma_h$ , while the neutral sector cross sections can be expressed in terms of the four preceding ones by the relationships

$$\begin{aligned} \sigma_{h3} &= \sigma_{h+} = \sigma_h \\ \sigma_{33} &= \sigma_+ + \sigma_- - \sigma_3 \\ \sigma_{hh} &= \sigma_+ + \sigma_- + \sigma_3 - 2\sigma_h \end{aligned} \quad (69)$$

The relations on the first line of eq.(69) are the simple  $SU(2)_V$  constraints already used in sec.2. The last one is obtained by straightforward algebra by using the eigenstate (65) on the  $\mathbf{T}_L = 1$ ,  $T_V = 0$  projectors (Appendix B).

The B-N violating corrections are finally found by assigning the Sudakov form factors (64) to each of the cross section combinations found before. We obtain

$$\begin{aligned} \sigma_+ + \sigma_- + \sigma_3 + \sigma_h &= \Sigma^H + 2\sigma_3^H, \\ \sigma_+ + \sigma_- + \sigma_3 - 3\sigma_h &= (\Sigma^H - 2\sigma_3^H) e^{-2\mathbf{L}_H}, \\ \sigma_+ - \sigma_- + 2I &= (\Delta^H + 2I^H) e^{-\frac{1}{2}(\mathbf{L}_W - \mathbf{L}_H)}, \\ \sigma_+ - \sigma_- - 2I &= (\Delta^H - 2I^H) e^{-2\mathbf{L}_W + \frac{3}{2}(\mathbf{L}_W - \mathbf{L}_H)}, \\ \sigma_+ + \sigma_- - 2\sigma_3 &= (\Sigma^H - 2\sigma_3^H) e^{-2\mathbf{L}_W + \frac{1}{2}(\mathbf{L}_W - \mathbf{L}_H)} \end{aligned} \quad (70)$$

from which each cross section can be derived.

## 6 Phenomenological Applications

Before applying the radiative corrections just found to some explicit phenomenological cases it is interesting to solve the systems (59) and (70), and to investigate their asymptotic limit  $\mathbf{L}_W \rightarrow \infty$ . In such a limit the values of the evolved cross sections - with radiative corrections - will depend only on some invariant combinations that do not evolve, i.e., are free of double-logs.

For the case with  $\sin\theta_W \neq 0$  and  $M_W \simeq M_H$  we have the two ‘‘invariants’’

$$\frac{\sigma_+ + \sigma_- + \sigma_h + \sigma_3}{4} \equiv \Theta_0; \quad \frac{\sigma_+ - \sigma_- + 2I}{4} \equiv \Theta_1 \quad (71)$$

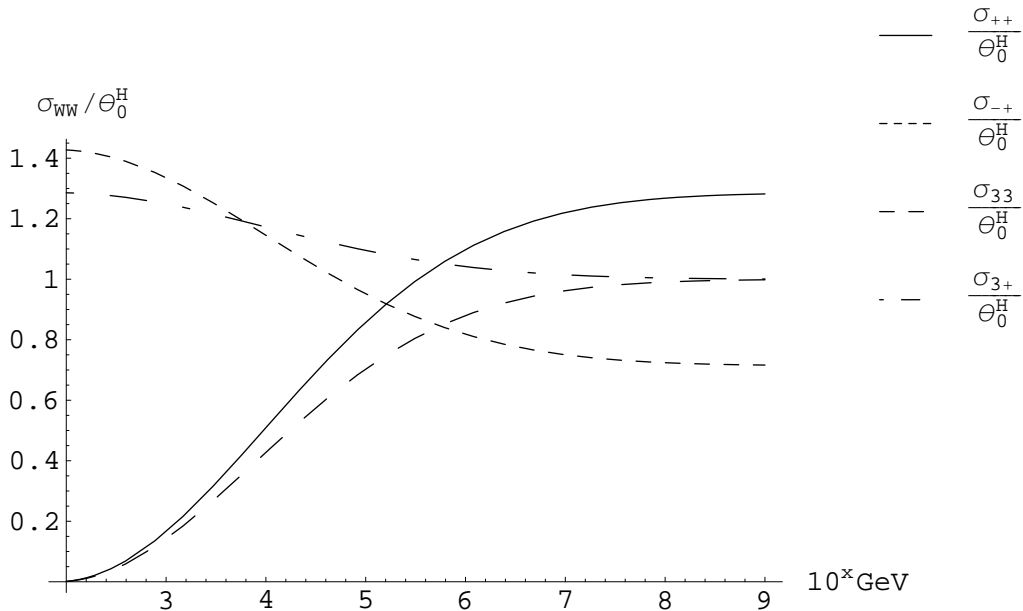


Figure 4:  $W_L W_L \rightarrow f \bar{f}$  inclusive cross section for  $M_W \simeq M_H$

with the constraint  $\sigma_h = \sigma_3$ . The first one corresponds to the cross-section average over the four Goldstone/Higgs states, and the second is the difference between the doublet and antidoublet averages. As a consequence, all cross sections converge to a combination of such two invariants:

$$\begin{aligned}
 \sigma_{\pm} &\rightarrow (\Theta_0^H \pm \Theta_1^H) \\
 \sigma_3, \sigma_{33} &\rightarrow \Theta_0^H \\
 I &\rightarrow \Theta_1^H \\
 \text{Re}\mathcal{O} &\rightarrow 0
 \end{aligned} \tag{72}$$

where the superscript  $H$  means that the invariants are evaluated at Born level.

For the case with  $\sin\theta_W = 0$  and  $M_W \ll M_H$  we also have the same two “invariants”, but now we find an extra  $M_H$  dependence in the limit  $\mathbf{L}_W \rightarrow \infty$  <sup>§</sup>:

$$\begin{aligned}
 \sigma_{\pm} &\rightarrow (\Theta_0^H \pm e^{-\mathbf{l}_h} \Theta_1^H) \\
 \sigma_3, \sigma_{33} &\rightarrow \Theta_0^H \\
 I &\rightarrow e^{-\mathbf{l}_h} \Theta_1^H
 \end{aligned} \tag{73}$$

Therefore, in the extra limit  $M_H \gg M_W$  all the physical cross sections would converge to the invariant  $\Theta_0^H$ , i.e., the average over all states.

The evaluation of the ratios  $\sigma_{ij}/\Theta_i^H$  give very easily an idea of the strength of the evolution of the cross section  $\sigma_{ij}$  under investigation. For instance, the cross section  $\sigma_{33}$  is of interest, because it can be identified in an  $e^+e^-$  collider by a double tagged experiment where the two final electrons both have transverse momenta  $|\mathbf{k}_{\perp}|^2 \gtrsim M^2$ . By eq. (59) it has the expression

$$\sigma_{33} = \frac{1}{4} [\Sigma^H + 2\sigma_{3+}^H + e^{-2\mathbf{L}_W} (\Sigma^H - 2\sigma_{3+}^H) + 2\text{Re}\mathcal{O}^H e^{-\mathbf{L}_W(2+\tan^2\theta_W)}] \tag{74}$$

in the case  $M_H \approx M$ , and an analogous one in the case  $M_H \gg M$ . The limit  $\sigma_{33} \rightarrow \Theta_0^H$  is obvious at large energies, while the full behavior depends on the explicit values of the Born cross sections.

Now let us discuss the example of  $W_L W_L \rightarrow$  hadronic jets. This cross section is relevant to describe hadron jet production at NLC by boson fusion, a process which becomes competitive with the annihilation process at high energies.

The Born cross sections for  $W_L W_L \rightarrow q\bar{q}$  are well known [18]:

$$\frac{d\sigma_{++}^H}{d\cos\theta} = \frac{d\sigma_{33}^H}{d\cos\theta} = 0 \tag{75}$$

<sup>§</sup> We stress that the limit that we are taking is  $\sqrt{s} \rightarrow \infty$  with  $M_H, M_W$  fixed. In such a case the combination  $\mathbf{L}_H - \mathbf{L}_W = -2\frac{\alpha_W}{4\pi} \log^2[M_H^2/M_W^2] \equiv -2\mathbf{l}_h$  is finite.

$$\begin{aligned}\frac{d\sigma_{3+}^H}{d\cos\theta} &= \frac{dI^H}{d\cos\theta} = \frac{\pi\alpha_W^2 N_c N_f}{8s} \frac{\sin^2\theta}{8} \\ \frac{d\sigma_{-+}^H}{d\cos\theta} &= \frac{\pi\alpha_W^2 N_c N_f}{8s} \frac{\sin^2\theta (9 - 18\sin^2\theta_W + 20\sin^4\theta_W)}{72\cos^4\theta_W}\end{aligned}$$

The corresponding evolution, e.g., for  $\sigma_{33}$  in the case  $M_H \approx M$  becomes, by eq. (74)

$$\sigma_{33} = \frac{1}{4}[\sigma_{-+}^H + 2\sigma_{3+} + e^{-2L_W}(\sigma_{-+}^H - 2\sigma_{3+}^H) - 2\sigma_{-+}^H e^{-L_W(2+\tan^2\theta_W)}] \approx \frac{1}{4}[\sigma_{-+}^H + 2\sigma_{3+} + \tan^2\theta_W \sigma_{-+}^H] 2L_W \quad (76)$$

In this case  $\sigma_{33}$  becomes nonvanishing for  $s > M^2$  because of radiative corrections, and  $\frac{\delta\sigma_{33}}{\Theta_0^H} \approx 2L_W$  is roughly of the order 10 % at the TeV threshold. This provides an estimate of the double logs, which are therefore of the same order as for fermions and transverse bosons initial states.

In Fig.4 we plot the ratios  $\sigma_{ij}/\Theta_0^H$  ( $\sin\theta_W \neq 0$ ,  $M_H \simeq M_W$ ,  $\cos\theta = 0$ ) over a huge energy range to show the ‘‘convergence speed’’ of the evolved cross sections.

In Fig.5 to the left we plot the same ratios as before but with three different  $M_H = 100, 500, 1000$  GeV cases ( $\sin\theta_W = 0$ ,  $M_H > M_W$ ,  $\cos\theta = 0$ ). To the right we plot the ratio between a cross section calculated with  $M_H = 100$  GeV over the same cross section calculated with  $M_H = 1000$  GeV to show the Higgs mass dependence as a function of the energy. This figure appears interesting from the Higgs physics point of view: while the hard  $WW \rightarrow f\bar{f}$  cross section is independent of the Higgs mass at high energies, the evolved ones instead show a pronounced effect coming from the exponential  $e^{-L_H}$  which tends to depress the corrections. This means that also completely inclusive cross sections not involving explicit Higgs production show enhanced Higgs mass dependence in their radiative corrections. Obviously, before bringing this simple example into the realm of phenomenology it needs many other inputs like luminosities of the longitudinal bosons, backgrounds etc. In any case we think that this extreme example can be useful to show the potential importance of this kind of ‘‘new Standard Model effects’’ related to the measure of inclusive cross sections at very high energy.

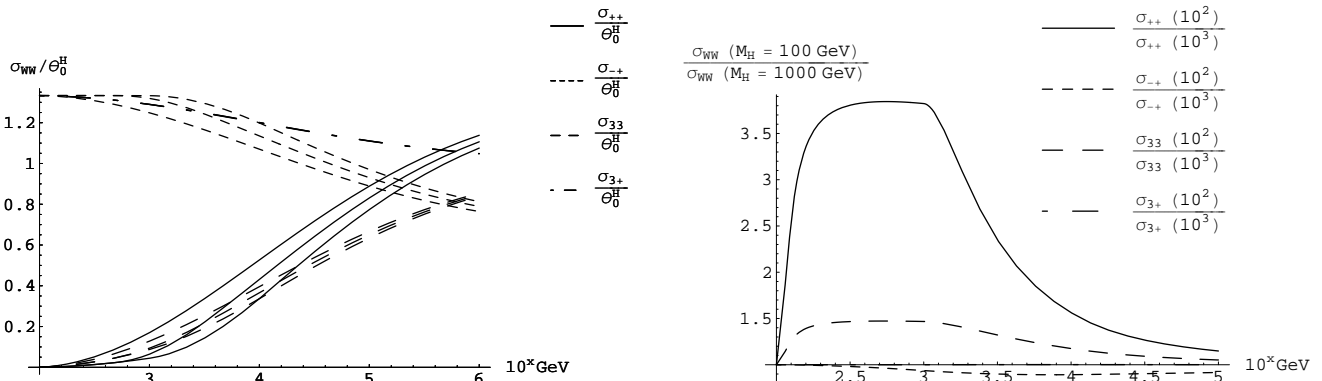


Figure 5:  $W_L W_L \rightarrow f\bar{f}$  inclusive cross sections for  $M_W < M_H$  and  $\sin\theta_W = 0$ . In the first picture to the left we show for three different values of  $M_H = 100, 500, 1000$  GeV the energy evolution of the cross sections. On the right we plot the energy dependence of the ratio between the cross sections calculated with  $M_H = 100$  GeV over the ones calculated with  $M_H = 1000$  GeV.

## 7 Conclusions

Our study of the longitudinal initial states occurring in boson fusion processes has shown that, in this case, enhanced radiative corrections have a number of interesting and sometimes surprising features.

First of all, soft interactions involve all four states of the Higgs sector, and this makes the group-theoretical classification of the corrections somewhat more involved than in previously analyzed cases (Sec. 2). We have provided here (Table 1) the combinations of cross sections with well defined form factors, for both  $M_H \approx M_W$  and  $M_H \gg M_W$ , and we have studied their radiative evolution.

Secondly, we find important *abelian* double logs [12], due to the breaking of weak hypercharge, besides the non-abelian ones. This is surprising at first sight, and is due to the occurrence of off-diagonal overlap matrix elements,

corresponding to a nontrivial hypercharge in the t-channel (eq. (59)). In turn, this happens because the longitudinal and Higgs states are mixed, i.e., are not hypercharge eigenstates.

Finally, the quantitative effects are sizeable, in the 5-10 % range at the TeV threshold as for the fermionic and transverse bosons initial states investigated previously. Furthermore, because of the enhanced radiative corrections, the Higgs mass dependence is not negligible (Fig. 5) even for processes without Higgs bosons in the final states, that are therefore insensitive to the Higgs mass at tree level.

On the whole, we have now provided a fairly complete description of the enhanced EW corrections for fermionic and bosonic initial states, which can now be used for detailed predictions of hard inclusive observables, at the double log level, at future accelerators energies. Of course, this is not enough: we actually need a generalization of collinear factorization to broken gauge theories, in order to account for single logarithms as well.

## 8 Appendix A: Soft Radiation Coefficients

Here we derive the expansions of the evolution coefficients  $\dot{L}_W$ ,  $\dot{L}_H$  and of their  $\tau$ -integrals for the explicit choice  $\tau = \omega$  and  $\tau = k_T$  of the evolution variable.

We start considering the effect of the collinear cutoff

$$\Theta_H = \Theta(2pk - M_H^2) \quad (77)$$

on one of the incoming momenta (either  $p = p_1$  or  $p = p_2$ ), and the corresponding calculation of the evolution hamiltonian in eq.(10).

By taking either  $\omega$  or  $k_T$  fixed the constraint (77) is written as

$$\frac{1}{\omega} \text{Max} \left( M, \sqrt{\frac{\omega}{M}} M_H \right) < \theta < 1, \quad (\tau = \omega) \quad (78)$$

$$k_T < \omega < \text{Min} \left( \frac{k_T^2 \sqrt{s}}{M_H^2}, \sqrt{s} \right), \quad (\tau = k_T) \quad (79)$$

By then integrating the eikonal radiator factor in eq.(10) over the region (78) we obtain ( $E \equiv \sqrt{s}$ )

$$\frac{\pi\tau}{\alpha_W} \dot{L}_H = 2 \log \frac{\omega}{M} \Theta(E M^2 - M_H^2 \omega) + 2 \log \frac{\omega E}{M_H^2} \Theta(\omega M_H^2 - M^2 E \omega) \quad (80)$$

for  $M < \tau = \omega < E$ , and

$$\frac{\pi\tau}{\alpha_W} \dot{L}_H = 2 \log \frac{E}{k_T} \Theta(k_T - M_H) + 2 \log \frac{k_T E}{M_H^2} \Theta(M_H - k_T) \quad (81)$$

for  $M < \tau = k_T < E$ ,  $E > M_H^2/M$ , while  $\dot{L}_W$  is given by the same expressions in the  $M_H = M$  limit.

Finally, by  $\tau$ -integration, we obtain in both cases

$$L_H = \frac{\alpha_W}{\pi} \left( \log^2 \frac{E}{M} - 2 \log^2 \frac{M_H}{M} \right), \quad E > \frac{M_H^2}{M} \quad (82)$$

which corresponds to eq. (62) in the text. In the intermediate energy region  $M_H < E < M_H^2/M$  we get instead

$$L_H = 2 \frac{\alpha_W}{\pi} \log^2 \frac{E}{M_H}, \quad M_H < E < \frac{M_H^2}{M} \quad (83)$$

as expected for a smooth  $E = M_H$  limit.

## 9 Appendix B

The overlap matrix can always be written as a sum of projectors  $\mathcal{O} = \sum C_i P_i$ . While the coefficients  $C_i$  depend on the dynamics and therefore on the physical process considered, the projectors  $P_i$  can be classified and explicitly constructed according to the relevant symmetry. We choose to classify the states according to their  $SU(2)_L \otimes SU(2)_R$  symmetry properties. This symmetry acts on the representation  $(\frac{1}{2}, \frac{1}{2})$  as follows:

$$(\bar{\Phi}\Phi) = \left( \begin{array}{cc} \bar{1} & 1 \\ 2 & 2 \end{array} \right) \rightarrow \exp[i\alpha_L^a \tau^a] (\Phi^c \Phi) \exp[-i\alpha_R^b \tau^b] \quad (84)$$

so that using the basis  $|t_L, t_L^3; t_R, t_R^3\rangle$  we can do the following identification:

$$|1\rangle = \left| \frac{1}{2}, \frac{1}{2}; \frac{1}{2}, \frac{1}{2} \right\rangle \quad |2\rangle = \left| \frac{1}{2}, -\frac{1}{2}; \frac{1}{2}, \frac{1}{2} \right\rangle \quad |\bar{1}\rangle = \left| \frac{1}{2}, \frac{1}{2}; \frac{1}{2}, -\frac{1}{2} \right\rangle \quad |\bar{2}\rangle = \left| \frac{1}{2}, -\frac{1}{2}; \frac{1}{2}, -\frac{1}{2} \right\rangle \quad (85)$$

Then the states coming from the direct sum  $T_L = t_L^1 + t_L^{1'}$  and  $T_R = t_R^1 + t_R^{1'}$  generate the representations  $(\frac{1}{2}, \frac{1}{2}) \otimes (\frac{1}{2}, \frac{1}{2}) = (0, 0) + (1, 0) + (0, 1) + (1, 1)$  that we label as  $|T_L, T_L^3; T_R, T_R^3\rangle$ . Explicitly, the states with  $(T_L, T_R) = (1, 1)$  are given by:

$$\begin{aligned} |1, -1; 1, -1\rangle &= |\bar{2}\bar{2}\rangle & |1, -1; 1, 0\rangle &= \frac{|\bar{2}\bar{2}\rangle + |\bar{2}2\rangle}{\sqrt{2}} & |1, -1; 1, 1\rangle &= |22\rangle \\ |1, 1; 1, -1\rangle &= |\bar{1}\bar{1}\rangle & |1, 1; 1, 0\rangle &= \frac{|\bar{1}\bar{1}\rangle + |\bar{1}1\rangle}{\sqrt{2}} & |1, 1; 1, 1\rangle &= |11\rangle \\ |1, 0; 1, -1\rangle &= \frac{|\bar{1}\bar{2}\rangle + |\bar{2}\bar{1}\rangle}{\sqrt{2}} & |1, 0; 1, 0\rangle &= \frac{|\bar{1}\bar{2}\rangle + |\bar{1}2\rangle + |\bar{2}\bar{1}\rangle + |\bar{2}1\rangle}{2} & |1, 0; 1, 1\rangle &= \frac{|\bar{1}2\rangle + |\bar{2}1\rangle}{\sqrt{2}} \end{aligned} \quad (86)$$

The states  $(T_L, T_R) = (1, 0)$  are:

$$|1, -1; 0, 0\rangle = \frac{|\bar{2}\bar{2}\rangle - |\bar{2}2\rangle}{\sqrt{2}} \quad |1, 0; 0, 0\rangle = \frac{|\bar{1}\bar{2}\rangle - |\bar{1}2\rangle + |\bar{2}\bar{1}\rangle - |\bar{2}1\rangle}{2} \quad |1, 1; 0, 0\rangle = \frac{|\bar{1}\bar{1}\rangle - |\bar{1}1\rangle}{\sqrt{2}} \quad (87)$$

while those  $(T_L, T_R) = (0, 1)$  are:

$$|0, 0; 1, -1\rangle = \frac{|\bar{1}\bar{2}\rangle - |\bar{2}\bar{1}\rangle}{\sqrt{2}} \quad |0, 0; 1, 0\rangle = \frac{|\bar{1}\bar{2}\rangle + |\bar{1}2\rangle - |\bar{2}\bar{1}\rangle - |\bar{2}1\rangle}{2} \quad |0, 0; 1, 1\rangle = \frac{|\bar{1}2\rangle - |\bar{2}1\rangle}{\sqrt{2}} \quad (88)$$

Finally, the singlet  $(T_L, T_R) = (0, 0)$  is:

$$|0, 0; 0, 0\rangle = \frac{|\bar{1}\bar{2}\rangle - |\bar{1}2\rangle - |\bar{2}\bar{1}\rangle + |\bar{2}1\rangle}{2} \quad (89)$$

In the  $M_H \simeq M_W$  case, the gauge symmetry  $SU(2) \otimes U(1)$  is the relevant one, and we can classify the states according to the  $(T_L, T_R^3 = Y)$  possible values; however this does not provide a complete classification of the states since  $U(1)_Y$  is an abelian symmetry. For instance, we have two states corresponding to  $T_L = 0, Y = 0$ ; one of them ( $|0, 0; 0, 0\rangle$  in eq. (89)) is CP-odd while the other ( $|0, 0; 1, 0\rangle$  in (88)) is CP-even. We can then use CP invariance to further classify the states, obtaining:

Eight ( $Y = 0$ ) states, whose multiplicity  $m$  is written in parenthesis:

$$|T_L, Y^2\rangle^{CP}(m) = |0, 0\rangle^-(1), \quad |0, 0\rangle^+(1), \quad |1, 0\rangle^-(3), \quad |1, 0\rangle^+(3) \quad (90)$$

Four ( $Y = 1$ ) and four ( $Y = -1$ ) states, which are interchanged by  $CP$  and must thus be degenerate:

$$|T_L, Y^2\rangle(m) = |0, 1\rangle(2), \quad |1, 1\rangle(6) \quad (91)$$

We have then 6 independent projectors, classified by their  $SU(2) \otimes U(1)$  and CP properties; 4 of them correspond to  $Y^2 = 0$  and are given in (90) and the remaining 2 with  $Y^2 = 1$  are given in (91). The subset of states corresponding to physical cross sections (with  $T_L^3 = Y = 0$ ) can be written in terms of the ones appearing in (86-89) as follows:

$$\begin{aligned} |T_L = 0, T_L^3 = T_R^3 = 0\rangle^+ &= |0, 0; 1, 0\rangle & |T_L = 0, T_L^3 = T_R^3 = 0\rangle^- &= |0, 0; 0, 0\rangle \\ |T_L = 1, T_L^3 = T_R^3 = 0\rangle^+ &= |1, 0; 1, 0\rangle & |T_L = 1, T_L^3 = T_R^3 = 0\rangle^- &= |1, 0; 0, 0\rangle \end{aligned} \quad (92)$$

Because of the mixing phenomenon in the neutral sector (see text), we also need the subset of (91) with  $Q = T_L^3 + T_R^3 = 0$  but  $Y = T_R^3 \neq 0$ :

$$|T_L = 1, T_L^3 = -1, T_R^3 = 1\rangle = |1, 1; 1, -1\rangle \quad |T_L = 1, T_L^3 = 1, T_R^3 = -1\rangle = |1, -1; 1, 1\rangle \quad (93)$$

In the  $M_H \gg M_W$  case we need classify the states according to their  $SU(2)_L \otimes SU(2)_R$  properties and their vectorial isospin  $\mathbf{T}_V = \mathbf{T}_L + \mathbf{T}_R$ . Writing them as  $|T_L, T_R; T_V\rangle$  we have then the possibilities:

$$|0, 0; 0\rangle \quad |0, 1; 1\rangle \quad |1, 0; 1\rangle \quad |1, 1; 0\rangle \quad |1, 1; 1\rangle \quad |1, 1; 2\rangle \quad (94)$$

The first three of them are given directly by eqs. (89,88,87), the states with  $T_L^3 = T_R^3 = 0$  corresponding to physical cross sections. The remaining three can be found by using the usual rules of isospin composition. It is relatively easy to find the states with  $Q = T_L^3 + T_R^3 = 0$ :

$$\begin{aligned} |1, 1; 0\rangle &\supset \frac{1}{\sqrt{3}}(|1, 0; 1, 0\rangle + |1, 1; 1, -1\rangle + |1, -1; 1, 1\rangle) & |1, 1; 1\rangle &\supset \frac{i}{\sqrt{2}}(|1, 1; 1, -1\rangle - |1, -1; 1, 1\rangle) \\ |1, 1; 2\rangle &\supset \frac{1}{\sqrt{6}}(-2|1, 0; 1, 0\rangle + |1, 1; 1, -1\rangle + |1, -1; 1, 1\rangle) \end{aligned} \quad (95)$$

## References

- [1] P. Ciafaloni, D. Comelli, Phys. Lett. **B446**, 278 (1999).
- [2] M. Beccaria, P. Ciafaloni, D. Comelli, F.M. Renard, C. Verzegnassi Phys. Rev. **D61**, 011301 (2000) and Phys. Rev. **D61**, 073005 (2000).



- [3] J.H. Kuhn, A.A. Penin, hep-ph/9906545.
- [4] E Accomando et. al., Phys. Rep. **299**, 1 (1998); Y.Sugimoto, KEK Proceedings-97-2.
- [5] P. Ciafaloni, D. Comelli, Phys. Lett. **B476**, 49 (2000).
- [6] V.S. Fadin, L.N. Lipatov, A.D. Martin, M. Melles, Phys. Rev. **D61**, 094002 (2000).
- [7] M. Ciafaloni, P. Ciafaloni, D. Comelli, Phys. Rev. Lett. **84**, 410 (2000), Nucl. Phys. **B589**, 359 (2000).
- [8] M. Ciafaloni, P. Ciafaloni, D. Comelli, Phys. Lett. **B501**, 216 (2001).
- [9] J.H. Kuhn, A.A. Penin, V.A. Smirnov, Nucl.Phys.Proc.Suppl. **89**, 94 (2000); Michael Melles hep-ph/0004056 and hep-ph/0012157; W. Beenakker, A. Werthenbach, Phys. Lett.**B489**, 148 (2000); M. Hori, H. Kawamura, J. Kodaira, Phys. Lett. **B491**,275 (2000).
- [10] R. Doria, J. Frenkel, J.C. Taylor, Nucl. Phys. **B168**, 93 (1980); G. T. Bodwin, S. J. Brodsky, G.P. Lepage, Phys. Rev. Lett. **47**, 1799(1981).
- [11] M. Ciafaloni, Phys. Lett. **B150**, 379 (1985); S. Catani, M. Ciafaloni, G. Marchesini, Nucl. Phys. **B264**, 588 (1986); M. Ciafaloni, in A.H. Mueller, Ed. "Perturbative Quantum Chromodynamics", 491 (1989).
- [12] M. Ciafaloni,P. Ciafaloni, D. Comelli, hep-ph/0103315.
- [13] M. Kopal, hep-ex/0102027; ALEPH Collaboration, Phys.Lett. **B495**,1 (2000).
- [14] B.I.Ermolaev, S. Fadin, JETP Lett.**23** 269 (1981); S. Fadin, Yad.Fiz. **36** N.8 (1982); A.H.Mueller, Phys. Lett. **B104** 161 (1981); A.H.Mueller,Nucl. Phys. **B213**, 85 (1983); **B228**, 251 (1983); Yu.L.Dokshitzer, S.I.Troyan, Proc. XIXth Winter School, LNPI 1984.
- [15] V.N. Gribov, Sov. J. Nucl. Phys. **5**, 399 (1967).
- [16] J.M. Cornwall, D. N. Levin, G. Tiktopoulos, Phys.Rev.**D10**, 1145,(1974), and Erratum-ibid.**D11**,972,(1975); B.W. Lee, C. Quigg, H.B. Thacker, Phys. Rev. **D16**, 1519 (1977); M.S. Chanowitz, M. K. Gaillard, Nucl. Phys. **B261**, 379 (1985).
- [17] Cf.,e.g., A. Dobado, M.J. Herrero, Phys. Lett. **B228**,495 (1989).
- [18] J. Layssac, F.M. Renard, G. Gounaris, Z. Phys. **C62**, 139 (1994).